Investigation of ultrasonic backward energy from various edges as a function of their 2D/3D geometry and of the incidence angle, for application to ultrasonic thermometry at the outlet of a tube

Marie-Aude Ploix, Gilles Corneloup, Joseph Moysan, Jean-Philippe Jeannot

Case Studies in Nondestructive Testing and Evaluation 6 (2016) 38–44

Contents lists available at ScienceDirect

Case Studies in Nondestructive Testing and Evaluation

www.elsevier.com/locate/csndt

Investigation of ultrasonic backward energy from various edges as a function of their 2D/3D geometry and of the incidence angle, for application to ultrasonic thermometry at the outlet of a tube

Marie-Aude Ploix [a,*], Gilles Corneloup [a], Joseph Moysan [a], Jean-Philippe Jeannot [b]

[a] Aix-Marseille Univ., LMA, CNRS, UPR 7051, Site LCND, IUT, Avenue Gaston Berger, 13625 Aix-en-Provence Cedex, France
[b] CEA Cadarache, DEN/DTN/STCP/LIET, 13108 St. Paul lez Durance, France

ARTICLE INFO

Article history:
Available online 30 September 2016

ABSTRACT

Innovative ultrasonic instrumentation to be used for future Generation IV sodium-cooled fast reactors is currently being investigated. One potential option under study here is the monitoring of the sodium temperature at the outlet of the core by using ultrasound. The main advantage of ultrasonic setups is that they can be used far from the intended subassemblies. The idea is to send an ultrasonic beam at grazing incidence towards the (cylindrical) subassembly head, and to measure the ultrasonic time of flight between the two diametrically opposite edges, in order to estimate the mean temperature across the subassembly outlet diameter. Moreover, the grazing incidence could allow considering the simultaneous temperature monitoring of several aligned subassemblies. One of the main points to be considered is the interaction between the ultrasonic beam and the immersed target, which involves specular reflection and/or diffraction, both phenomena depending on the incidence angle and the target geometry. The present paper investigates this interaction, mainly from an experimental point of view. Different geometries of "2D" (plate) and "3D" (tube) edges are tested and compared under various incidence angles. The final aim is to identify an optimal ultrasonic configuration to perform thermometry at the outlet of an immersed tube.

1. Introduction and context

In the general topic of designing new sodium-cooled reactors [1], some innovative solutions for monitoring the structure are being investigated in order to improve the performances of the periodic and continuous control [2,3]. In particular, an ultrasonic configuration aiming at monitoring the temperature of the liquid sodium at the outlet of the fuel subassemblies (see Fig. 1a) is being examined. Based upon a British patent [4], the idea is to measure the time-of-flight of the backward echoes reflected (or diffracted) by the diametrically opposite edges of the targeted cylindrical subassembly (see Fig. 1b). The knowledge of the (empirical) relationship linking sodium temperature with ultrasonic velocity [5] allows estimation of

* Corresponding author.
E-mail address: marie-aude.ploix@univ-amu.fr (M.-A. Ploix).

http://dx.doi.org/10.1016/j.csndt.2016.09.001

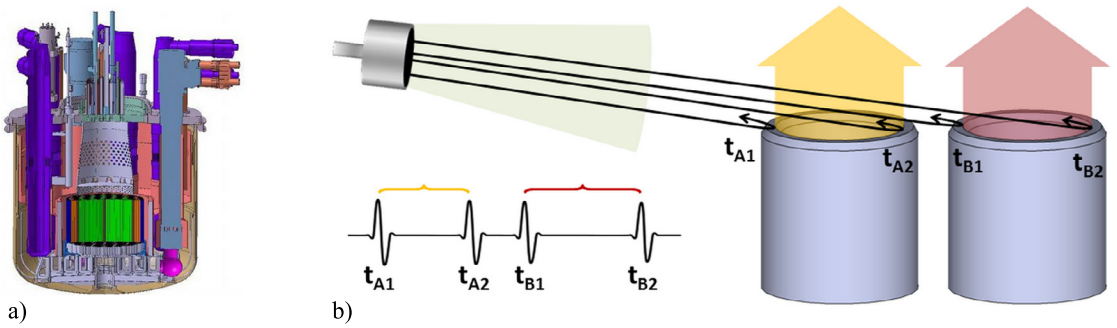

Fig. 1. a) Example (section) of design of sodium-cooled reactor: core (subassemblies) is the green area, b) setup idea at the top of the core: (t_{A2}–t_{A1}) and (t_{B2}–t_{B1}) depend on the flow temperature outing each tube.

the mean temperature on the diameter of the tube outlet. Moreover, if the incident beam is sufficiently grazing to insonify several aligned subassembly outlets it should be possible to monitor several subassemblies simultaneously.

The influence of the fluid thermodynamic variations (flow and temperature heterogeneities) in this area is also under study, but independently (see details in [6,7]), and therefore will not be taken into account here. In particular, these works showed that (1) the flow has a weak influence as far as ultrasonic propagation is quite perpendicular to the flow direction, (2) the measure provides the average temperature on the diameter of the tube end, and (3) the sensitivity is about 1% of the nominal liquid sodium operating temperature. We aim here at a deeper study of the ultrasonic setup including the tube end geometry and machining to optimize the temperature measurement signal to noise ratio in the static case.

The echoes from the edges of an immersed target can be due to two different phenomena: specular reflection and/or diffraction. The diffraction effect induces complex scattered fields, depending on the geometry of the edge and on the incidence of the ultrasonic beam. Several theories to model this phenomenon can be found in the literature, among which the Geometrical Theory of Diffraction (GTD) [8], based on the ray theory. Another approach particularly used in the case of complex target shapes is the Kirchhoff approximation [9]. Other theories [10,11] mainly aim at improving the accuracy and the limits of classical methods. B. Lü et al. [12] proposed a combination of GTD and Kirchhoff approximation: the authors developed the so-called refined Kirchhoff approximation by employing GTD diffraction coefficients (model implemented in CIVA software [13], used in the following). All these studies concern 2D theoretical considerations, and to the author's knowledge, no experimental work has been published.

The purpose of this study is three-fold: (1) to analyse and compare the different edge geometry influences, (2) to analyse experimentally the impact of 2D/3D geometry, (3) finally to identify an optimal configuration (edge geometry and incidence angle) for the purpose of monitoring several aligned targets. The definition chosen here for the "optimal configuration" is based on the working assumption that the time-of-flight will be more accurately measured if the signal-to-noise ratio is maximal. To have a good signal-to-noise ratio, high backscattered signals are essential, and so the aim will be here to maximize the signal amplitude. The choice of the best method of time-of-flight measurement (peaks, zero-crossing, correlation, ...) may then be considered on these optimized signals.

For the experimental measurements, liquid sodium was replaced by water under ambient conditions in view of similarities between these two media [14] – particular their close acoustic impedances: about 1.5 MPa s/m for ambient water, and 1.9 MPa s/m for sodium at 550 °C [5] (about 45 MPa s/m for the steel of plates and tubes noted for reference). Note that for future sodium applications, specific high temperature transducers are currently available and qualified, and new generations are under development (see [15] for more details).

2. Diffraction from 2D edges

The first geometry investigated is a "2D" geometry with plates of various edge shapes. Experiments and modelling are performed, analysed, and compared.

2.1. Plates and ultrasonic setup

Two 20 mm thick stainless steel plates have been specially and accurately milled, providing four different plate edges (Fig. 2): right-angle, fillet, 45°-chamfer and 60°-chamfer. Ultrasonic measurements are performed by immersion in water. The flat ultrasonic transducer (1″-diameter, broadband, 2.25 MHz centre frequency) is first adjusted so that the incident beam is initially normal to the front face of the plate, at a distance of 250 mm (the plate is in the early far field of the transducer). Then the transducer position is tilted in the XZ plane, from 0° to 15° with 1°-increment (and an extra measurement performed at 30°). For each fixed tilt angle, the transducer scans the Z-axis while registering signals (0.5 mm-step).

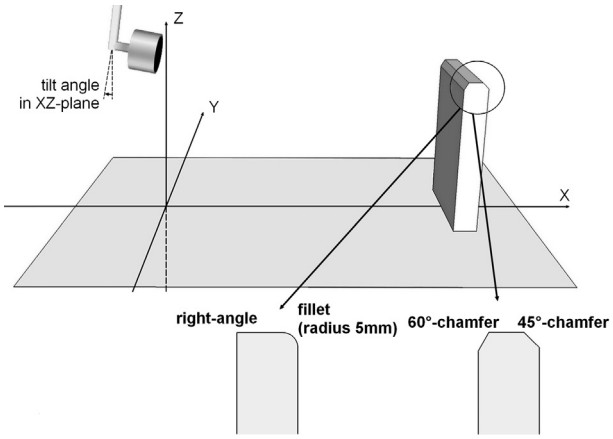

Fig. 2. Experimental setup and edge geometries.

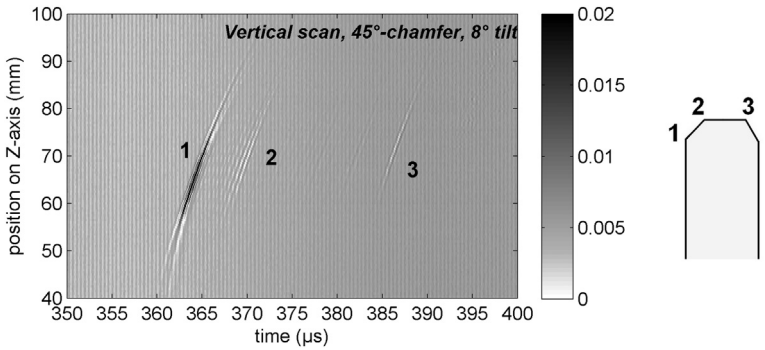

Fig. 3. Absolute amplitudes acquired vertically on 45°-chamfer, at 8°-tilt.

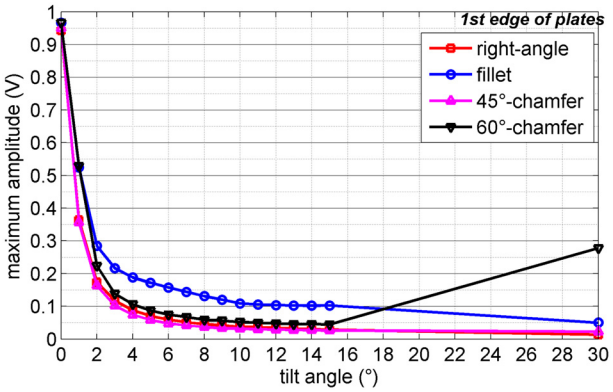

Fig. 4. Registered maximum amplitudes from the four different plate edges.

2.2. Results and analysis

Every tilt angle provides a set of signals for the different altitudes of the transducer. These signals can be visualized through an amplitude image, as shown in Fig. 3. The first interesting observation is the diffraction echoes from all the "visible" edges (see example on Fig. 3).

Fig. 4 represents the resulting maximum amplitudes of the first echo over all Z-positions, as a function of the tilt angle, for each geometry. As expected, there is a rapid decay of amplitude when tilting the angle from normal incidence. Indeed, normal incidence generates specular reflection of the entire beam from the face of the plate, whereas non-perpendicular incidence implies diffraction, thus less energy returning to the transducer.

Right-angle and chamfer geometries send back similar amplitudes all over the range of tilt angles, except for 60°-chamfer at 30°-tilt, which corresponds to the normal incidence to the chamfer plane (the surface of the "insonified" 60°-chamfer

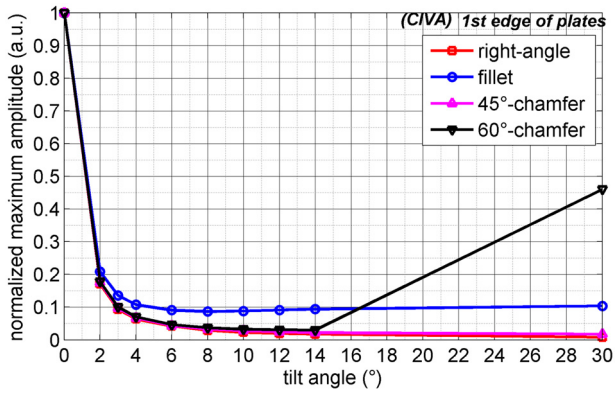

Fig. 5. Simulated maximum amplitudes from the four different plate edges.

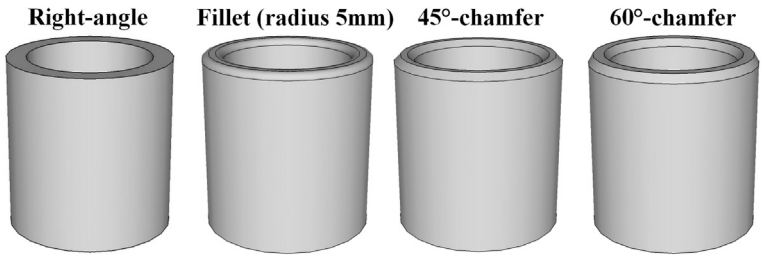

Fig. 6. Tubes with various edge geometries.

plane at 30°-tilt is about one third of the sound field cross section, which explains the difference in specular energy between 0° and 30°). The fillet edge reflects more energy than the other edge configurations by a factor of approximately 2. Indeed, this geometry involves specular linear reflection on a curved edge rather than diffraction on an angled corner, which may explain the difference in amplitude.

2.3. Comparison to modelling

CIVA software [13] is a ray theory based software modelling tool that has been used for 2D ultrasonic diffraction modelling [12,16,17] principally to simulate defect responses. In this application, CIVA was used to simulate the edge responses.

The simulation configuration and procedure exactly reproduce the experimental configuration and procedure described above. As previously, the resulting (normalized) maximum amplitudes are plotted as a function of the tilt angle (Fig. 5).

The modelled amplitudes clearly confirm the experimental ones:

- The amplitudes returned by the different plate edge geometries markedly decrease with the increase in the tilt angle, and become quite stable from about 10°-tilt.
- The 60°-chamfer produces a specular reflection for 30°-tilt because a part of the beam is at normal incidence to the chamfer.
- The right-angle geometry and chamfers reflect the same amplitudes (except 60°-chamfer at 30°-tilt), while the fillet sends approximately twice as much energy back to the transducer.

3. Diffraction from 3D edges

The same analysis is performed on so-called “3D” edge geometries, that is to say here the internal and external (convex and concave) edges of tubes. Only the experimental study is reported, because 3D diffraction is not implemented in CIVA.

3.1. Setup and configuration

Four tubes have been specially produced (15 mm wall thickness and 95 mm internal diameter), their edge geometries being the same as the plate edge geometries: right-angle, fillet, 45°-chamfer, and 60°-chamfer (see Fig. 6). Internal and external edges at the upper ends of the tubes, whether concave or convex, have identical geometries.

The 3D experimental setup is identical to the 2D setup: the tube is positioned in the early far field (at 250 mm) of the ultrasonic transducer, which is initially set at normal incidence to the curvature of the tube (which is in the symmetry plane of the tube) and scans the Z-axis for the different fixed angles of tilt.

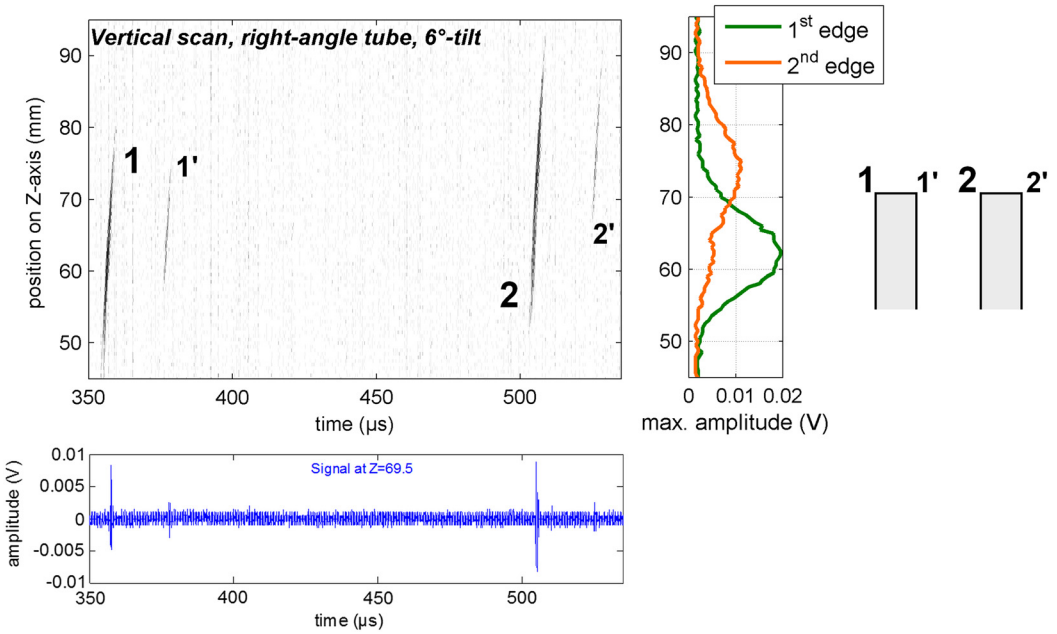

Fig. 7. Example of experimental acquisition (right-angled tube, 6°-tilt): (left) greyscale image of amplitude versus time and transducer altitude (with extracted signal at $Z = 69.5$ mm in blue), and (right) selected amplitudes from each edge denoted 1 and 2.

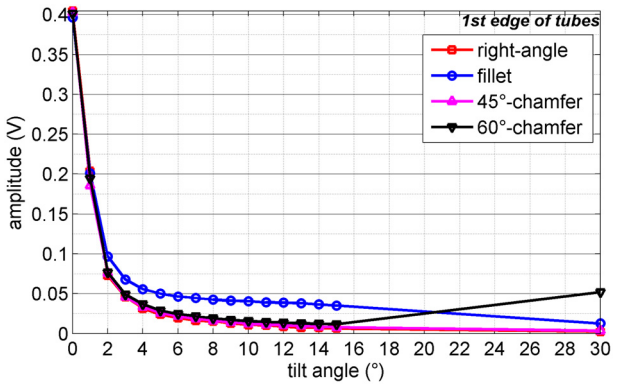

Fig. 8. Registered maximum amplitudes from the convex edges.

In this configuration, there are two echoes of interest: one corresponding to the diffraction from the convex, external edge, the first to be impinged upon, denoted “1” in Fig. 7, which shows an example of acquired data, and one corresponding to the diffraction from the concave, internal edge, denoted “2” in Fig. 7. Both echoes are clearly identifiable and can be processed individually.

3.2. Amplitudes returned by each edge

The amplitudes of the signals diffracted by each individual edge are first processed and analysed separately. The maximal amplitudes of the backward signals from the first, convex edge of each tube are plotted as a function of the tilt angle (Fig. 8). The curves exhibit a behaviour very similar to that for the 2D plates. Right-angle and chamfers provide the same amplitudes, and the fillet reflects roughly twice as much energy. The absolute amplitudes are approximately three times smaller than the plate edge amplitudes.

The amplitudes of signals sent back by the second, concave edge of each tube are plotted in Fig. 9. The low tilt angles (up to about 5°) induce low amplitudes: indeed this edge is almost invisible because hidden behind the first one and thus the beam cannot reach it. Then, above 5°, the behaviour is similar to that for the convex edges: the fillet reflects more than twice the amplitude of the other geometries. The absolute amplitudes are here two times smaller than those from the first, convex edge.

There is a clear difference between these results and those for the 2D plates. The convex/concave nature of the edges is certainly partly responsible for the amount of energy returned to the transducer. The loss of amplitude can also be partly

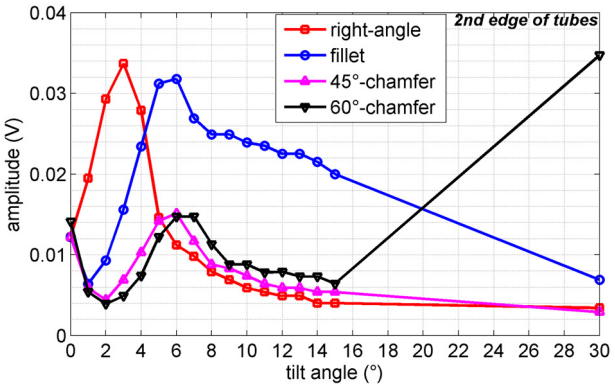

Fig. 9. Registered maximum amplitudes from the concave edges.

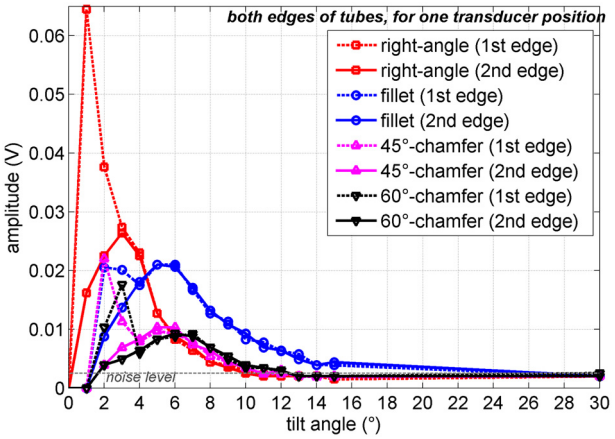

Fig. 10. Registered maximum amplitude from the tube edges for a single position of the transducer.

due to the larger distance travelled by the ultrasound propagating in water, and thus due to the influence of the aperture of the beam.

3.3. Amplitudes returned by both edges simultaneously

The intended application implies "seeing" both edges simultaneously, for one transducer position (that is, one angle and one altitude). Indeed, as instantaneous measurement is what is aimed at, scanning is not conceivable. The transducer needs to be at an optimal position (here, altitude) to get from both targets the "best signals" at the same time, for post-processing. These "best signals" are those with the highest possible amplitudes from both edges at one transducer position.

Identifying the optimal position consists then here in finding the transducer altitude for which both edges send back a maximum of energy. So a compromise is made between the amplitudes sent back by each edge: for each given transducer altitude Z, the smaller of both amplitudes is selected, and the maximum of this value over all Z positions is chosen as optimal. As an example: on Fig. 7, the highest possible amplitudes from both edges simultaneously (for this geometry and this tilt angle) are registered at the altitude of the transducer of 69 mm, which is then identified as the optimal altitude.

The resulting amplitudes are plotted in Fig. 10. First of all, one can see that when the condition of simultaneity is added, the large amplitude at 30°-tilt for the 60°-chamfer disappears. Likewise, amplitudes are null at 0°-incidence: there is no transducer altitude for which both edges are visible (the second edge is always hidden by the first one).

The two chamfered tubes present similar, rather low optimal amplitudes, with a maximum for a tilt angle of about 6°. The tube with fillets presents a maximum at 5°, and the amplitude is twice that for chamfers. The right-angled tube proves to be the best geometry in terms of maximum amplitude (at 3° tilt).

4. Conclusions

The present work optimizes the configuration in terms of edge geometry and ultrasonic tilt angle to obtain the highest signal amplitude back from a tube end. The simulated and experimental results for the 2D configuration (with plates) show that the fillet geometry sends back the highest signal amplitude over a large angular range. This is logical from a theoretical

point of view (predominant specular reflection rather than diffraction, involving a more energetic return to the transducer), and consistent with the simulations performed with CIVA software.

The 3D measurements on tubes confirm the results obtained for the 2D plates: they show that the fillet edges reflect more energy when observed individually. However, when the transducer is positioned so that both edges can be observed at the same time, neither of them is ideally observed, and the best geometry in terms of backscattered signal amplitude is the right-angled edge. Fillets remain however good candidates for intended applications on tubes, as they produce a wider angular range of large amplitudes sent back to the transducer, allowing uncertainties on the transducer tilt angle. These results will contribute to academic discussion about the need to develop 3D numerical simulations for an accurate understanding of wave propagation.

The final objective is to measure the fluid temperature at the outlet of a subassembly by ultrasound. Thus further investigations will be required before real application in a reactor, in particular concerning the accuracy of the measurement, in the static case and then with the complex thermohydraulic conditions at the outlet of the core. Different parameters may interfere with the ultrasonic measurement at varying degrees, such as the possible uncertainty on the relative location of the edges (dilatation…) and on the position of the transducer, the signal processing chosen to estimate time-of-flight, or the variations of flow...

The work presented in this article fits perfectly into the new notion of "RC-CND" (*Recommendations de Conception issues du Contrôle Non Destructif*, that is, design recommendations resulting from Non Destructive Testing) currently developed in the French nuclear industry [18]. These recommendations apply to the design of objects or structures not only considering its mechanical aspects but also in conjunction with the future NDT objectives.

Moreover, this kind of ultrasonic configuration can also be used for various other applications, as in telemetry, to monitor target positions, or dilatation measurements, etc. Moreover, the grazing nature of the optimal geometry and acoustical configurations presents two significant advantages: firstly a limited impact of fluid outflow on wave propagation (ultrasonic waves almost perpendicular to the flow), and secondly the obvious potential of simultaneous measurements for several aligned objects with only one transducer.

Acknowledgement

This research work was supported by CEA Cadarache.

Appendix A. Supplementary material

Supplementary material related to this article can be found online at http://dx.doi.org/10.1016/j.csndt.2016.09.001.

References

[1] Gauche F. Generation IV approach – the development of sodium fast reactors. Magnetohydrodynamics 2012;48:191–5.
[2] Jadot F, Baque F, Jeannot JP, de Dinechin G, Augem JM, Sibilo J. ASTRID sodium cooled fast reactor: program for improving in service inspection and repair. In: 2011 2nd int. conf. adv. nucl. instrum. meas. methods their ppl.. 2011. p. 1–8.
[3] Jeannot JP, Rodriguez G, Jammes C, Bernardin B, Portier JL, Jadot F, et al. R&D program for core instrumentation improvements devoted for French sodium fast reactors. In: 2011 2nd int. conf. adv. nucl. instrum. meas. methods their appl.. 2011. p. 1–7.
[4] McKnight JA, Macleod ID, Burton EJ. Ultrasonic beams. http://www.google.com/patents/US4655992 (accessed August 22, 2014).
[5] Sobolev V. Database of thermophysical properties of liquid metal coolants for GEN-IV. SCK•CEN, Mol, Belgium. http://hdl.handle.net/10038/7739, 2011.
[6] Massacret N, Moysan J, Ploix MA, Jeannot JP, Corneloup G. Modelling of ultrasonic propagation in turbulent liquid sodium with temperature gradient. J Appl Phys 2014;115:204905. http://dx.doi.org/10.1063/1.4875876.
[7] Nagaso M, Moysan J, Benjeddou S, Massacret N, Ploix MA, Komatitsch D, et al. Ultrasonic thermometry simulation in a random fluctuating medium: evidence of the acoustic signature of a one-percent temperature difference. Ultrasonics 2016;68:61–70. http://dx.doi.org/10.1016/j.ultras.2016.02.011.
[8] Keller JB. Geometrical theory of diffraction. J Opt Soc Am 1962;52:116. http://dx.doi.org/10.1364/JOSA.52.000116.
[9] Zernov V, Fradkin L, Darmon M. A refinement of the Kirchhoff approximation to the scattered elastic fields. Ultrasonics 2012;52:830–5. http://dx.doi.org/10.1016/j.ultras.2011.09.008.
[10] Pierce AD, Hadden WJ Jr. Plane wave diffraction by a wedge with finite impedance. J Acoust Soc Am 1978;63:17–27. http://dx.doi.org/10.1121/1.381709.
[11] Berg P, If F, Nielsen P, Skovgaard O. Diffraction by a wedge in an acoustic constant density medium. Geophys Prospect 1993;41:803–31.
[12] Lü B, Darmon M, Potel C, Zernov V. Models comparison for the scattering of an acoustic wave on immersed targets. J Phys Conf Ser 2012;353:12009. http://dx.doi.org/10.1088/1742-6596/353/1/012009.
[13] Calmon P, Mahaut S, Chatillon S, Raillon R. CIVA: an expertise platform for simulation and processing NDT data. Ultrasonics 2006;44:E975–9. http://dx.doi.org/10.1016/j.ultras.2006.05.218.
[14] Grewal S, Gluekler E. Water simulation of sodium reactors. Chem Eng Commun 1982;17:343–60. http://dx.doi.org/10.1080/00986448208911637.
[15] Baque F, Reverdy F, Augem JM, Sibilo J. Development of tools, instrumentation and codes for improving periodic examination and repair of SFRs. Sci Technol Nucl Install 2012:718034. http://dx.doi.org/10.1155/2012/718034.
[16] Dorval V, Chatillon S, Lü B, Darmon M, Mahaut S. A general Kirchhoff approximation for echo simulation in ultrasonic NDT. In: Rev. prog. quant. nondestruct. eval., vols. 31a, 31b. AIP conf. proc., vol. 1430. 2012. p. 193–200.
[17] Lü B, Darmon M, Fradkin L, Potel C. Numerical comparison of acoustic wedge models, with application to ultrasonic telemetry. Ultrasonics 2016;65:5–9. http://dx.doi.org/10.1016/j.ultras.2015.10.009.
[18] Corneloup G, Gueudré C, Ploix MA, Augem JM, Sibilo J, Lebarbé T, et al. Recommandations de Conception issues du Contrôle Non Destructif (RCC-MRx). Bordeaux, France, http://www.ndt.net/article/cofrend2014/papers/ME2D3_G_CORNELOUP.pdf, 2014.